A Progress Report:

DESIGN AND APPLICATION OF ELECTROMECHANICAL ACTUATORS FOR DEEP SPACE MISSIONS

Submitted to:

NASA
Marshall Space Flight Center EP64
ATTN: Rae Ann Weir

Prepared by:

Dr. Tim A. Haskew
Assistant Professor
Department of Electrical Engineering

Dr. John Wander
Assistant Professor
Department of Mechanical Engineering

College of Engineering
The University of Alabama
Box 870286
Tuscaloosa, AL 35487-0286

Reporting Period:

8/16/92 - 2/15/93

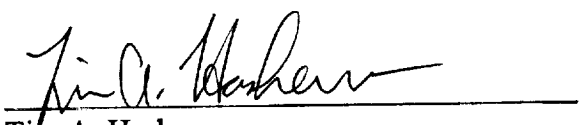

Tim A. Haskew
Project Director, Co-Principal Investigator

John Wander
Co-Principal Investigator

I. INTRODUCTION

This progress report documents the efforts on the grant entitled "Design and Application of Electromechanical Actuators for Deep Space Missions," which is grant number NAG8-240, during the period 8/16/92 through 2/15/93. During this period, work has been focused on three major topics:

1) Screw Modeling and Testing
2) Motor Selection
3) Health Monitoring and Fault Diagnosis

Detailed theoretical analysis has been performed to specify a full dynamic model for the roller screw. A test stand has been designed for model parameter estimation and screw testing. In addition, the test stand is expected to be used to perform a study on transverse screw loading. With regard to construction of the test stand, we are faced with the question of equipment/manufacturing funding. We hope to entertain this question at a future meeting with NASA personnel.

In the area of motor selection, we are seeking to provide responses to each of the primary vendors reasons for their motor selection. In addition, we are forming our own bases and guidelines for motor selection. Simulations are being performed to rank the candidate machines based upon our selection criteria.

Work on the topic of health monitoring and fault diagnosis is also in progress. We are currently investigating a software filter to read measured system data and provide an output that will contain estimates of some of the noisy system measurement quantities as well as several system model parameters. It is expected that these estimates can be used to predict and classify impending failures.

The following individuals constitute the EMA research group:

1) Tim A. Haskew*, Project Director, Co-Principal Investigator
   Assistant Professor, Department of Electrical Engineering
2) John Wander*, Co-Principal Investigator
   Assistant Professor, Department of Mechanical Engineering
3) Thomas E. Salem*
   M.S. Student, Department of Electrical Engineering
4) Stuart Payne*
   M.S. Student, Department of Mechanical Engineering
5) Ramomohan Challa
   M.S. Student, Department of Computer Science
6) Sumit Bhattacharyya
   M.S. Student, Department of Electrical Engineering

Those individuals marked with an asterisk (*) are actually appointed to positions funded through the grant. The others are working on topics strongly related to the overall effort, but receive no tuition or salary support out of grant funds.

We feel that substantial progress is being made. One major reason is that NASA personnel, namely Rae Ann Weir and John Sharkey, have been extremely helpful and willing to provide information as needs arose. As a result, we expect to soon be engaging in technology transfer through the publication of our results and approaches in various technical journals and conference proceedings.

This report is intended simply as a progress report. The annual report at the end of this first full grant year is expected to provide a complete and highly detailed description of the year of work. Three report sections follow this introduction. In each, specific details on the progress made on each of the three major topics of study are provided.

II. PHASE 1 TASK I.1: ROLLER SCREW MODEL AND TEST STAND DEVELOPMENT

Any physical system can be modeled in a variety of ways depending on the purpose of the model and the desired accuracy. An even greater variety of models is possible if variations in the physical system are considered. Since the roller-screw-based actuators will be designed differently for different applications, a wide variety of models is possible. It is therefore helpful to discuss some of the design choices involved in linear actuator development and the impact those choices can have on system behavior.

II.1. Roller Screw Design Choices

Roller, ball, or lead screws are commonly used to transform rotary motion into linear motion. As in any transmission design, the mechanical advantage or gear reduction, and the bearing design have direct impact on overall system capabilities. When space applications are considered, several additional considerations must be made including thermal energy management and higher reliability requirements. The vacuum environment of space poses special long-term problems for some lubricants and can cause much higher rates of molecular bonding between bearing surfaces. Various issues that should be considered when making specific roller screw design choices for space applications are discussed in the following.

II.1.1 Transmission Ratio

The most basic design choice for a linear screw corresponds to the most basic model of this device: the ratio between angular and rotary motion. This choice should properly be viewed as only part of the overall transmission ratio between the prime

mover (electric motor for an EMA) and the output linear motion. When the screw is part of a mechanism, the additional nonlinear transmission between linear motion and the output motion of the mechanism should be considered. The effects of this design choice are very broad. Determining which effect should govern the choice of this parameter requires consideration of the specific application. Some of the obvious considerations are the inertia being scaled by the square of the transmission ratio, the torque-speed curve being scaled by the transmission ratio, and the mission energy requirement which will be altered by both the effective inertia and the effective torque-speed curve as well as the screw efficiency that depends on transmission ratio. For TVC, one should consider the effective inertia of the actuator as seen from the engine nozzle as well and the more standard effective inertia seen by the motor. Startup transient loads can be greatly affected by this effective inertia.

One measure of the quality of a linear screw is the degree to which the simple transmission ratio expression for the relationship between angular position and linear position captures the actual behavior or the device:

$$X = P_h\theta \tag{II.1}$$

In Eq. II.1, X represents the linear displacement of the screw, P_h is the screw lead, and θ is the angular shaft displacement. An improved kinematic model of the screw includes the deviation from an exactly linear relationship between X and θ:

$$X = P_h\theta + f(\theta) \tag{II.2}$$

In Eq. II.2, $f(\theta)$ represents the deviation from a linear relationship between X and θ. The SKF Group will supply this function as a set of discrete measurements upon request. An example of this data is shown on page 5 of their roller screw catalog [II.1]. This example indicates a mean deviation of approximately $2.5\ 10^{-6}$ m ($9.8\ 10^{-5}$ in). This deviation is smaller than the $7.6\ 10^{-4}$ m accuracy required of the typical TVC application. The decision to model this deviation will depend on the functional requirements placed on the roller screw. For example, if $|f(\theta)|$ is small compared

with the required accuracy or if there is linear position sensing available, the deviation term may be unimportant. On the other hand, if $f(\theta)$ is of significant magnitude in comparison to the accuracy required and no linear position sensing is available (or one wishes to use angular position sensing as a backup method of positioning in case of linear sensor failure) this term may be critical. The design specification for an upper limit on the magnitude of $f(\theta)$ can eliminate the need for a model in the form of Eq. 2 for some applications. On the other hand, as the accuracy requirement of a given application increases, it may become impossible to hold a manufacturing tolerance tight enough to allow $f(\theta)$ to be neglected in the system model.

In addition to the manufacturing errors that contribute to variations in the lead, both temperature variation and loading can generate errors that might be viewed as errors in lead. These issues are discussed further below.

II.1.2 Bearing Design

The roller screw and actuator must be designed to bear the applied load through structural members and across moving bearings. The perspective most often taken with this aspect of design is to avoid failure by yield or fatigue. The accuracy and stiffness of moving bearings is often increased by preloading at the expense of efficiency and bearing life. The SKF literature indicates a clear tradeoff between a nonlinear stiffening spring rate associated with unpreloaded bearings and an increasing nonlinear dry friction (preload torque) associated with increasing preload (see Figure 5 in the SKF catalogue). While these types of nonlinearities have long been a challenge to servo control designers, the preload may pose additional difficulties in vacuum where the bearing surfaces are likely to bond. Research associated with the SP100 space reactor project has shown significant bearing surface welding in vacuum conditions [II.2]. The dwell time at a given position was shown to have a strong affect on friction

coefficient. This result has serious implications for long-duration space applications. New surface treatment methods may offer a solution to this problem [II.3].

From a load bearing perspective, a roller screw can be viewed as an axially loaded member that is changing length and hence stiffness. This changing stiffness can also be a challenge to a servo designer and may lead to column buckling. Considering bearing stiffness and changing load path length, the compliance of the roller screw is a nonlinear function of load and an approximately linear function of screw extension. The amount of variation in stiffness can be controlled by selection of the preload and the crossection of the members in the changing load path.

One aspect of actuator design with roller screws is support of the reaction torque. The actuator can be designed to support this torque internally or to have the reaction torque supported by the clevis connections to the environment. Because earlier hydraulic TVC designs did not require reaction torque support through their environmental connections, it is likely that internal reaction torque support will be easier to implement in TVC retrofits of EMAs. Internal support is generally a more independent design but may lead to vacuum welding problems.

Another feature of linear screw design is the requirement that loading be primarily axial in nature. Pierre Lamore of SKF has said that the transverse loading on the nut must be kept to less than 10% of the axial load. While it seems reasonable that this means 10% of the rated axial load, he seemed to indicate 10% of the actual axial load. This interpretation is supported by the need to ensure proper symmetrical location of the rollers. Because the actuator may experience high accelerations transverse to its axis, significant transverse nut loading may occur for some actuator designs. Given the general actuator bearing design shown in Figure II.2, and assuming that the moments generated by individual bearing contacts are negligible, it is possible to evaluate the side loading applied to the nut due to actuator acceleration in a direction transverse to the actuator.

The actual transverse load on the nut is a function of a wide variety of parameters including N, the acceleration of the vehicle in g's, and the extension of the actuator. The following analysis is based on the Honeywell actuator though exact values for most of the parameter values are not known. Using the system model shown in Figure II.1 the transverse loading shown in Figure II.2 is produced. While it is possible to shield the nut from bearing these loads, a simpler and more compact design results if some of this load can be borne by the nut. Investigation of the transverse load bearing capabilities of roller screws seems warranted.

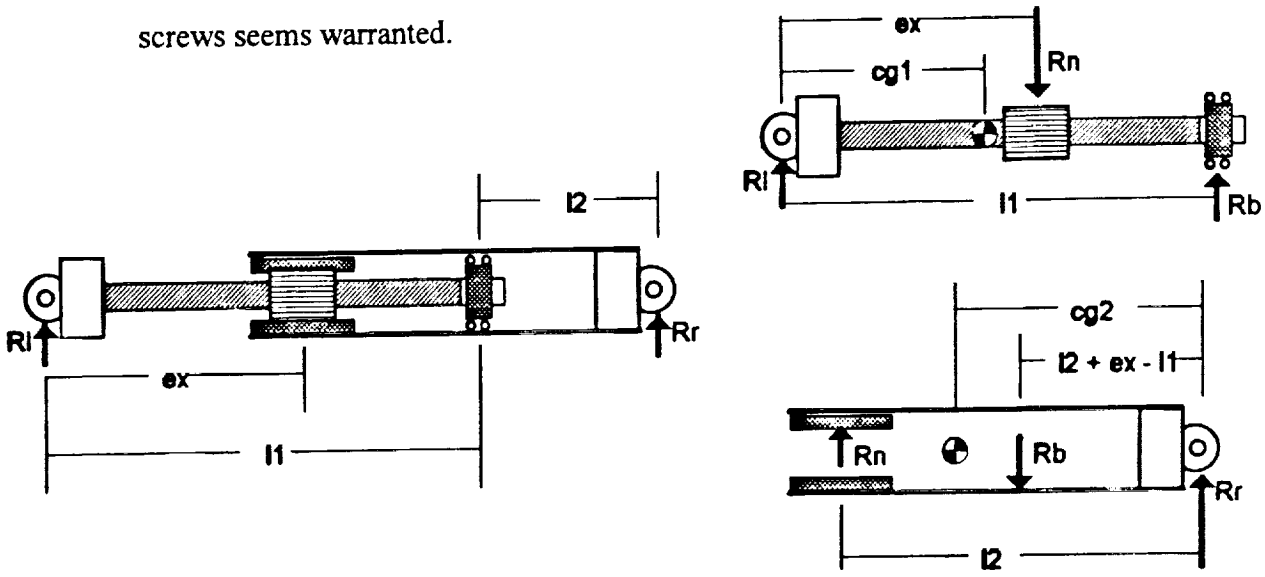

Figure II.1. TVC Actuator Schematic for Transverse Loading Analysis.

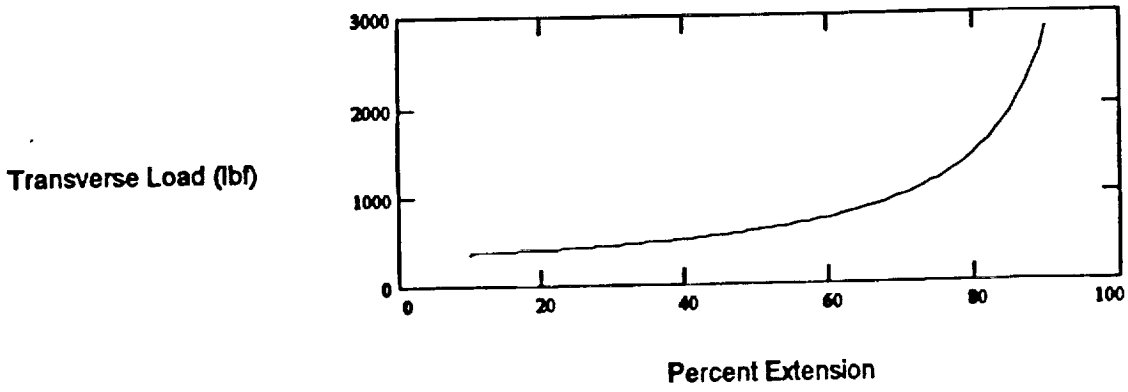

Figure II.2. Peak Transverse Nut Loading of TVC Actuator.

II.1.3 Thermal Energy Management

Of some concern is the effect of temperature on screw performance. Little in the way of research on this subject has been found. One group published experimental and theoretical work with the thermal expansion of a ball screw nut [II.4]. The thermal time constant of a standard industrial roller screw is roughly an hour. Temperature changes cause variation in frictional behavior and the screw length. In a cyclic test with a preloaded nut, a 30 to 45 % reduction in frictional torque is accomplished over a 3 to 4 hour period due to the changing viscosity of the lubricant. With the dry lubricants likely to be used in space this effect will be reduced. The change in length of the screw was found to be well predicted by the average temperature multiplied by the coefficient of thermal expansion. Thermal expansion will definitely effect the lead of the screw with SKF suggesting shaft extension of
$11.5\ 10^{-6}$ m/m-^{o}C.

II.1.4 Failure Modes

The various design considerations mentioned above lead one to speculate about the various failure modes that might occur with a roller screw. Column buckling and bearing fatigue failure seem the most likely considerations. Attempts to minimize rotary inertia may lead to high slenderness ratio screws while bearing damage may be accelerated by vacuum welding. In addition, the transverse loading condition mentioned in connection with TVC may cause bearing failure. Similarly, the engine startup transients may cause bearing damage and subsequent failure. Given a single screw to convert angular to linear motion, a roller screw represents a single-point failure mechanism for an EMA built around it. It might be possible to expand the roller screw design, however, to include an annular double nut to provide for coaxial

redundant conversion of rotary to linear motion as shown in Figure II.3. With this concept, only the inner transmission would be normally used and the outer nut would be held fixed with respect to the piston. If the rollers or races associated with the inner nut were damaged, it could be locked with respect to the screw becoming part of the screw and the piston housing with its internal threads would become the active nut.

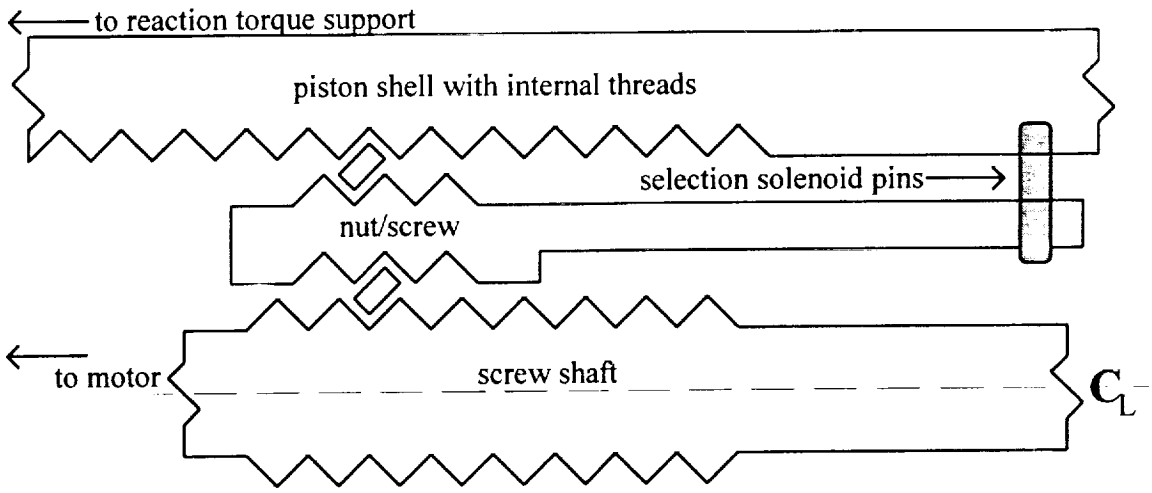

Figure II.3. Dual Nut & Screw Design for Redundant Screw.

The above discussion is meant to give a quick overview of the design issues involved in selecting a linear screw as part of an EMA. Table II.1 lists the important design features and the associated issues. Each of the tradeoffs should be considered in light of their impact on performance and failure modes.

TABLE II.1 Roller Screw Design Issues

Design Feature	Relevant Issue: Prime Mover			Mission Requirements			Reliability/Failure	
	Power	Torque	Energy	Accel. / Vel. / Load	Accuracy	Endurance	Structural	Redundancy
Transmission Ratio	√	√	√	√	√	√		
effective inertia		peak accel.		accel.		accel. load		
kinematic scaleing	peak vel.			vel. & load	resolution	cycle, load		
efficiency			loss/cycle			heating		
Bearings	√	√	√	√	√	√	√	√
type, size				load limit	stiffness	fatigue, weld	yield	number
materials, treatment						fatigue,weld	yield	
preload	torque	torque	torque		backlash	fatigue,weld		
Heat Management	√	√	√	√	√	√	√	
expansion					lead	therm. stress		
lubrication			low fric.					
temperature	elec. resist.	elec. resist.	elec. resist.				weakening	

II.2. Roller Screw Model Development

The previous discussion suggests a variety of behaviors that might be included in a roller screw model as part of an EMA for space application. A simple transmission ratio may suffice in some cases where parameter variation as a function of temperature, position, dwell time and load may be required in other cases. The following sections outline a variety of models to be pursued and experiments to be performed.

II.2.1. Inertia Model

Purely kinematic models of the roller screw as given in Eqs. II.1 and 2 above can be used to generate an effective load inertia at the prime mover. The contribution of the screw inertia itself can also easily be added. Assuming a straight connection between the linear motion of the screw and the load mass, an inertial model based on a constant screw lead would be

$$I_{eff} = I_m + I_t + G_r^2 I_s + (G_r P_h)^2 (M_n + M_l) \qquad \text{(II.3)}$$

where:

- G_r is the gear reduction between motor and screw shaft,
- P_h is the lead of the roller screw,
- I_m is the rotor inertia of the motor,
- I_t is the transmission inertia referred to the motor rotation,
- I_s is the effective rotary inertia of the screw shaft and rollers,
- M_n is the mass of the nut and attached hardware, and
- M_l is the mass of any driven load.

The determination of the parameters in this model and the addition of any mechanism transmission can all be easily and analytically accomplished with good accuracy. Thus, a reasonably accurate rigid-body inertia model can be determined without experiment. If a

function $f(\theta)$ as indicated in Eq. II.2 is to be used for the screw, Eq. II.3 can be modified with the derivative of this function in place of the lead, P_h.

A consideration of the above inertial model for the two-motor NASA TVC actuator under development at MSFC indicates that the effective inertia of the SME nozzle dominates all other system inertias. Adopting parameter values: load mass 300 slugs, motor inertia 4*0.00043 in-lb-s^2, screw inertia 0.0077 in-lb-s^2, lead = 10 mm, and gear reduction 8.875/1, the effective inertia of the load referred to motor rotation is roughly thirty times the next most important inertia (that of the motors).

II.2.2. Compliance Model

A first model of compliance as a simple linear spring constant modulated by screw position can be readily formulated. In a significantly preloaded situation, the cumulative effect of the bearings in the system will contribute a constant compliance term in addition to the term linear in screw extension. In an unpreloaded situation, the deflection as a function of load might have the form:

$$\delta = C_b F^{1/3} + C_x (X_o + X) F \qquad \text{(II.4)}$$

where:

- δ is the total axial deformation in the screw system,
- C_b is the stiffening spring compliance associated with the roller bearing,
- C_x is the compliance per unit length of the screw shaft,
- X_o is a constant that generates the fixed compliance associated with zero screw extension ($C_x X_o$ produces a deflection term linear in F), and
- X is the extension of the screw.

In this model the cubed root was adopted in conformance with the common practice of using a 3rd-order function of displacement to model a stiffening spring force. Another coefficient might easily be determined from experimental data derived from static

force/deflection tests. One might even hope to predict the first natural frequency of axial vibration or limit cycling with this model under certain situations.

More exact models that include multiple modes of deflection or explicitly include transverse loading effects can be envisioned. At this point, however, the most important aspect of transverse loading seems to be the potential inducement of bearing failure.

II.2.3. Friction Model

The frictional behavior of a roller screw is generally regarded to be of a stick-slip nature: applied torques below the preload torque generate no velocity. This behavior becomes critically important when trying to achieve very high accuracies [II.5, 6]. Traditional models of friction behavior (such as the well-known Tustin model) may capture large-scale motion very well while failing entirely to predict small-scale behavior. Numerical models of stick-slip behavior that include microscopic compliance in parallel with the friction displacement have made it easier to simulate frictional behavior on both the macroscopic and microscopic levels. The "reset integrator" model recently published by Haessig [II.7], for example, has been used by the author to develop high-fidelity models of stick-slip behavior in robot axes [II.8]. Once the stick-slip behavior can be reproduced by such a model, nonlinear control techniques can be used to generate high-accuracy positioning while avoiding limit cycles.

Experiments to determine the parameters for a stick-slip model require application of known torques while monitoring motion in the joint. The best data is obtained if accelerations are measured. As mentioned earlier, temperature and exposure to vacuum can have a large effect on frictional behavior. As a first level of control, such experiments should be performed at a controlled temperature in earth atmosphere. Later, if desired, attempts can be made to explicitly include temperature and vacuum exposure and dwell time to the model.

II.2.3. Transverse Loading

Though a physically based model for the bearing wear as a function of transverse loading is not immediately desired, it is important that some measure of the wear due to transverse loading be obtained. It may seem that a roller screw capable of supporting a 45,000 lbf axial load ought to be able to support a 2000 lbf transverse load, but comments by SKF personnel have left this author uncertain. Therefore it is planned to apply transverse loads to a roller screw in excess of the maximum expected transverse TVC load with a variety of axial loads (including zero axial load) and move through a number of motion cycles that far exceed the TVC requirement. It is hoped that subsequent inspection of the screw will show no appreciable wear. Previous attempts to generate bearing failure have led to unacceptably long-duration experiments [II.9].

II.2.3. Axial Shock Loading

As indicated earlier, the engine startup transient can produce significant side loads on the nozzle. This loading has been described as a 100,000 lbf momentary loading on the TVC actuator. For the purpose of this investigation, this description is interpreted to mean the load experienced by the screw nut if it is prevented from moving during the transient. In addition to concerns over plastic deformation of the basic actuator structure, there is concern that the screw bearings will be permanently deformed or weakened by the transient. For this reason, experiments involving such temporary shock loads are planned to determine the effects on the screw bearings.

Another approach to transient loading could be taken. If the startup transient is brief in duration, it may be possible to avoid large actuator loads by having the TVC actuator to

comply (actively or passively) with the nozzle motion. Regardless of the method chosen, experiments to demonstrate the response to shock loading will be conducted.

II.3. Roller Screw Test Stand Design

A general-purpose test stand has been designed to allow the above outlined experiments to be performed. This test stand can be used with a roller screw in isolation or an entire TVC or other actuator. The following section provides a set of specifications for the computer control of this system and a brief description of the test device.

II.3.1 Computer Control and Data Acquisition System

A variety of control and data acquisition system possibilities were considered with cost and system adaptability of prime importance. The computer requirements for the various tests to be performed differ widely. Simple static compliance tests could be performed without computer control while experimentation with active compliance to shock loading requires both high-speed control and data acquisition. With this variety of requirements and the possibility of additional requirements associated with still undefined experiments, it was decided to use a PC buss for which the widest variety of peripherals are inexpensively available. Compromising between desired experimental capabilities and hardware abilities, the following specifications have been developed:

- 20 channels of differential A/D (25 kHz sampling on each of 4 channels)
- simultaneous sampling on at least 4 channels, preferably 8
- 4 channels of simultaneous analog output
- 3 channels of digital parallel I/O
- controlled system sampling period

At this time, peripheral products by National Instruments and Computer Board Inc. are being compared for the best mix of capabilities. The entire system design including system control software should be completed in April, 1993.

II.3.2 Bearing Frame and Instrumentation

In order for the roller screws to be properly tested and the mathematical models properly developed, a test stand has to be designed and built. This experiment stand must be versatile to allow for a variety of experiments. Significant effort has been expended to anticipate potential experiments and allow for easy modification of the test stand.

Design Criteria

The following represents the basic design criteria of the test stand as determined by various mission specifications and modeling requirements:

- Transient Loading Of Up To 100,000 lbf
- Able To Support Multiple Experiments
- Adaptability For Future Experiments
- Side Loading
- Variable Coupling To Motors And Screws
- Ability To Approximate Actuators
- Capable Of Housing An Entire Actuator
- Ability To Be Placed In A Controlled Environment

The test stand design was based on all of these requirements. However, particular emphasis was placed on adaptability.

Preliminary Considerations

First and foremost, the stand had to bear the 100,000 lbf shock loading used to simulate engine startup transients. In order to simplify the design procedure and incorporate a factor of safety, the 100,000 lbf transient loading was considered to be a static load of 200,000 lbf. Support of this load requires significant structural members.

Since large structural members were required, it was considered best if the stand was a frame like structure constructed in the horizontal plane. Figure II.4 shows the preliminary design of the test stand. It can be seen from Figure II.4 that the many devices that have to be attached to the stand provide for an accessibility problem. It was decided that a test bed width of 36 inches would provide enough room for easy access to all the different components, while not being too large as to cause space allocation problems. The test bed internal span length was designed to be variable from a maximum of 72 inches to a minimum of 24 inches. This provides for much flexibility in the types of roller screws that can be tested.

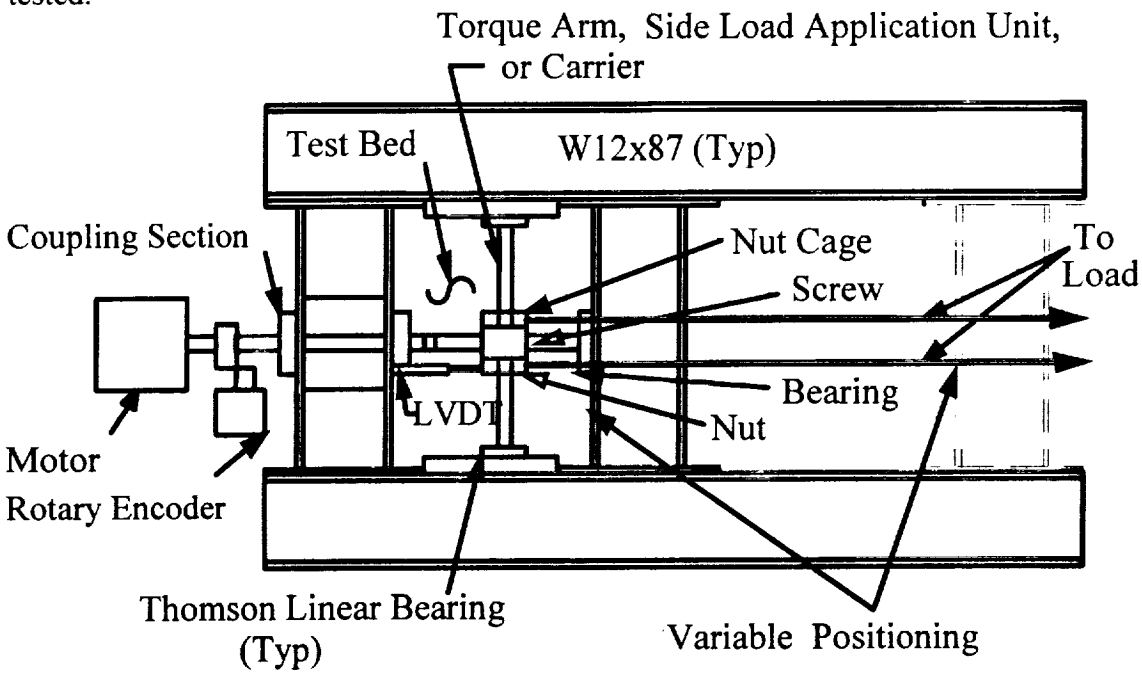

Figure II.4. Scale Drawing of Roller Screw Test Stand

Structural Member Selection

With the preliminary size constraints known, the calculations for the proper size structural members could be made. The resulting structure is statically indeterminate and required the use of Castigliano's theorem for analysis. Castigliano's theorem is a relatively simple method for determining deflections and reactions in a structure [II.10]. The equations

obtained from Castigliano's theorem were used to determine the proper size members for failure due to yield. The resulting structural members are W12x87's, which provide adequate strength to protect against failure at all critical points.

Connection Design

Once the proper frame members were selected, the connections had to be designed. A four tension bolt end-plate connection [II.11] was chosen for its strength and simplicity. This design resulted in the use of a 3/4 inch thick end plate in conjunction with twelve one inch diameter A490 bolts and four 3/4 inch thick stiffeners. The end plates are welded to the ends of the cross members which are then bolted to the longitudinal members. This design allows the test fixture to have a variable test bed length since it is bolted together and not welded.

Motor and Screw Coupling Section

With the basic frame in place, the next step was to design a coupling system that would withstand the required loading and be flexible enough so as to accommodate different motors and screws. Since different tests would require different loading conditions, it was necessary to have a system that was capable of bearing both axial and radial loads. This was accomplished by using both a spherical roller bearing and a tapered roller bearing. This combination, shown in Figure II.5, is capable of handling high loads for short periods of time and moderate loads for a long periods of time. The advantages of this system can easily be seen from the figure. The locations of the bearings make access to them relatively easy, while the integration of the structural member into the assembly allows for a very high load bearing capability.

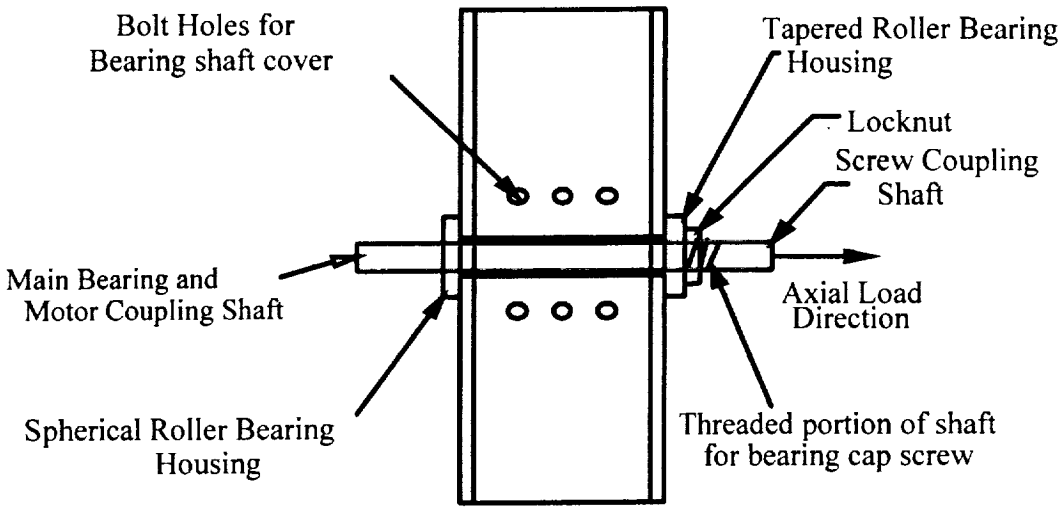

Figure II.5. Coupling System

As previously mentioned this system requires two bearings for a proper working configuration. This is due to the fact that the spherical roller bearing requires a minimum load of 20 lbf. This minimum load can be achieved by placing a tapered roller bearing on the opposite flange of the structural member and using a threaded locknut to hold the bearing in place. In this way the shaft at the point of the tapered roller bearing can be threaded and the locknut can be tightened down until the desired minimum load is achieved. This extra bearing also provides for added stability for the coupling shaft.

Linear Bearing System

Another integral part of the basic design for this test fixture was to closely approximate the different actuators that might be used. For thrust vector control, the nut rides in a carrier while one end of the screw is unsupported. One way to achieve this configuration is to use two linear bearing systems that act as carriers for the nut. In this way the two systems restrict the nut's rotation while allowing it to travel in the axial direction, thus closely approximating the actuator for thrust vector control. This system is shown in Figure II.6.

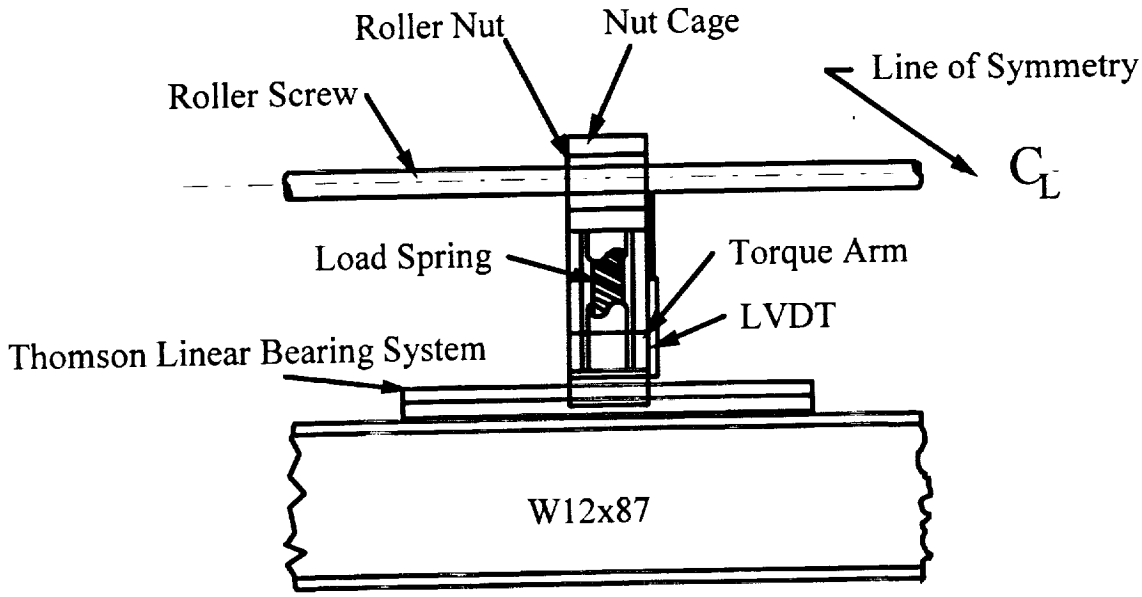

Figure II.6. Linear Bearing System

These linear bearings can have many different functions depending upon the type of experiment being conducted. They can serve as the platform for applying side loads during the transverse loading experiments. They can also be used as a platform for measuring large torques produced by the nut. This can be accomplished by using the carrier arm in conjunction with a load cell as a dynamometer. In addition to the aforementioned uses, the linear bearing system could also be used to carry a LVDT that would measure transverse deflections.

Transverse Loading Experiment

This particular experiment requires that side loading be applied to the actuator. The side load will be applied using a spring loaded system that will be carried by one of the linear bearing systems. This system is represented, except for minor differences, in Figure II.6 above. The difference between the figure and the actual system is that there is only one linear bearing system used. As the previous statement implies, this means that the nut will not be carried by the linear bearings, instead the roller screw will be supported by an additional tapered roller bearing located at the variable end of the test bed.

Other requirements of this test include measuring the transverse deflections of the screw and the torque seen by the nut. The transverse deflections of the screw will be obtained by simply mounting a LVDT on the linear bearing perpendicular to the screw. Also, if large enough, the torque seen by the nut will be measured by using a torque arm and load cell combination in a dynamometer configuration (see Figure II.6). However, if the resultant torques are too small to be practically measured by the torque arm, an in-line torque sensor will be used.

Friction Experiment

For the friction experiments, the key factors are the measurement of rotary and axial displacements, and torque. For the rotary displacement measurements, it will be necessary to use a rotary encoder geared from the main shaft. For the axial displacement measurement, a LVDT will be mounted as shown in Figure II.4. Also, for the torque measurements, an in-line torque sensor will be used since the associated torque will be small.

Transient Loading Experiments

In order for these experiments to be conducted, a system for loading the actuator will have to be developed. It is envisioned that a flywheel and clutch or a weight and mechanical advantage system will be used to provide the impulse. It is felt that the weight and mechanical advantage system will provide the simplest and most cost effective design. This system will be connected to the actuator via cables attached to the nut cage (See Figure II.4.). The impulse seen by the nut can be shaped by the distance of drop, weight, and cable stiffness. Also, these loads will need to be measured. This will require placing rod-in-line threaded load cells at the point of load application.

Flexibility for Future Experiments

Not all experiments can be envisioned at this time, however, the features of this test fixture were designed to provide the maximum flexibility for future use. Such features

include bolted components and connections, space for additional components, allowance for variable positioning of the test bed, and a multipurpose coupling system that allows for the use of many different types of motors and actuators.

Summary

As can be seen from this report, this test stand provides for many different experiments, both seen and unseen. It is believed that sufficient forethought was incorporated into the design so as to limit any future modifications to only minor changes in the stand. Another aspect of this design is that it allows for the placement of an entire actuator in the test bed, and yet it still retains the capability of being placed in controlled environments.

A breakdown of the required individual parts and their associated costs is given in Table II.2. Some of the parts listed in the table are still tentative choices, however, they provide a good estimate of part inventory and cost. As the design stands, the total cost for the frame structural materials, instruments, and assembly is $10,000. This estimate does not include the cost of the system to generate the shock loading or the cost of the computer control system.

Table II.2. Summary of Test Stand Parts and Costs.

Item Description	Part Number	Number Required	Cost Per Item	Total Cost	Figure Reference
Structural Members	W12x87	22 Ft.	$25/Ft.	$550	??.1
Spherical Roller Bearing	(SKF) 29412E	1	$380	$380	??.2
Tapered Roller Bearing	(Timken) 476,472	2	$50	$100	??.2
Thomson Linear Bearing	1CC-16-HAA L18	2	$620	$1240	??.2
Torque Arm Load Cell	(Sensotec) AL131	2	$400	$800	N/A
Thrust Load Cell	(Sensotec) AL417	1	$700	$700	N/A
In-Line Torque Sensor	(Sensotec) BT111	1	$1250	$1250	??.1
LVDT's (Sensotec)	BY126HQ, BY127HV	1 1	$330 $640	$330 $640	??.3 ??.1
Rotary Encoder	?	?	?	?	??.1

II.4 References

[II.1] SKF Planetary and Recirculating Roller Screws, Catalogue 3793 U.S., SKF Group, 1990.

[II.2] Dalcher, Alfred W. et. al., "Development Testing of High Temperature Bearings for SP-100 Control Drive Assemblies," Ninth Symposium on Space Nuclear Power Systems, Albequerque, NM, January 12-16, 1992.

[II.3] "State of the Art Hard-Coatings", Manufacturing Applications and News, January, 1993, pp. 12-14.

[II.4] Otsuka, J., S. Fucada, and N. Obuchi, "Thermal Expansion of Ball Screw and Its Theoretical Analysis," ASME paper 84-DET-205.

[II.5] Ro, P. and P. Hubbel, "Model Reference Adaptive Control of Dual-Mode Micro/Macro Dynamics of Ball Screws for Nanometer Motion," to appear in the March 93 issue of ASME Journal of Dynamic Systems Measurement and Control.

[II.6] Ro, P. and P. Hubbel, "Nonlinear micro-dynamic behavior of a ball-screw driven precision slide system," Precision Engineering, October 1992, Vol. 14, No. 4, pp. 229-236.

[II.7] Hassig, David A. and Bernard Friedland. "On the Modeling and Simulation of Friction," Proc. 1990 American Control Conference, pp. 1256-1261, 1990.

[II.8] Wander, J. Development of Robot Deflection Compensation for Improved Machining Accuracy, Ph.D. Dissertation, The University of Texas at Austin, 1990.

[II.9] McCool, John, I., "Life of Concentrated Contacts in the Mixed EHD and Boundary Film Regimes," Final Report, NAPC-PC-204C, for the Naval Propulsion Center, August, 1989.

[II.10] Shigley, Joseph E., and Charles R. Mischke, Mechanical Engineering Design, Fifth Edition, New York: McGraw-Hill Publishing Company, 1989, pp. 112 - 120.

[II.11] Manual for Steel Construction, Allowable Stress Design, Ninth Edition, "Four Tension Bolt End-Plate Design Procedure," Chicago: American Institute for Steel Construction Inc., 1989.

III. MOTOR SELECTION: THRUST VECTOR CONTROL APPLICATIONS

The focus of this chapter is to evaluate existing machine technologies for their applicability in use for the electromechanical actuation (EMA) in Thrust Vector Control applications. Attention will first be given to defining the motor selection criteria, then a review of vendor proposals is offered, followed by a discussion on simulation studies used to evaluate the motor options.

III.1. Selection Criteria

There are numerous standard industrial selection guidelines when choosing an electric motor for a particular job application. These criteria have been reviewed with respect to the thrust vector control application. Guidelines such as cost and power source requirements are beyond the scope of this research effort. Other criteria, such as physical size and weight, do not prove to be distinctive for selection primarily due to the advances in motor technology. The guidelines which will be used for this research are listed below:

1. Reliability - the performance dependability of the motor,
2. Controllability - an accuracy measurement of motor control response to command input,
3. Torque production characteristics - including starting torque, torque-speed relationship, torque fluctuation, step load change response, and maximum torque capability,
4. Efficiency - the measurement of usable mechanical output power versus supplied electrical power input, and
5. Thermal considerations - motor performance in various temperature regions and machine heating due to electrical losses.

Due to the nature of the application, reliability becomes the most important consideration, and all other criteria will be considered with respect to reliability. The EMA system reliability may be sub-categorized into components, and the current research work focuses only on the evaluation of motor reliability. To enhance the overall reliability of the EMA system, motor redundancy has been assumed for the selection evaluation.

Since motor performance is typically listed by manufacturers in an optimum fashion, i.e. efficiency is normally listed for rated running conditions; the emphasis will be to evaluate the selection criteria during a specified operating sequence. This type of analysis should provide a more realistic appraisal of the performance characteristics of the motors for their anticipated load cycles. Failure mode analysis will also be used as a critical evaluation tool. All of the guidelines will be analyzed for performance during a faulted condition of one of the motors in the redundant set.

III.2. Overview of Vendor Proposals

Several Vendors have submitted proposals for electromechanical actuation systems in thrust vector control applications. This is not an exhaustive review of all available submittals; for example, Honeywell has not been included in this survey since the details of their proposal have not been received.

III.2.1. General Dynamics

General Dynamics has proposed the use of induction machine technology for EMA applications [III.1]. As stated, their choice was not based on 'the usual trade parameters (mass, volume, cost, etc.)', since the motors under consideration do not gain distinction

from these criteria [III.1]. Instead, the proposal seems to be based on the following considerations:

1. Torque-speed performance for step load changes,
2. Failure mode analysis for redundant motor system, and
3. Thermal considerations.

These criteria address several important issues primarily dealing with how the machines will respond during a motor failure in a redundant system. A couple of items of concern are raised about the performance ability of the brushless permanent magnet technology within this scenario. First of all, if the motors are operating near rated speed during the failure, the brushless machine will slow down significantly to meet the increased torque production requirements. The induction machine, on the other hand, will only slow down slightly in order to pick up the additional load. This drastic speed change is sighted as a substantial problem for the permanent magnet motor. Additionally, if the motor failure is the result of a short circuit forming in the stator windings of the machine, the faulted permanent magnet motor will act as a generator thus supplying energy to the fault which will be consumed as heat. This generator action will not occur for the induction machine.

III.2.2. Allied Signal

Allied Signal has proposed the use of the brushless permanent magnet machine technology for EMA systems operating in temperature regions less than 200_ C, and the induction machine technology for applications in higher operating temperature regions [III.2]. Efficiency, torque production characteristics, and thermal considerations appear to be among the main selection criteria. Brushless machine technology is the preferred choice for its higher efficiency rating, proven application history and system robustness. However, it is important to note the thermal limitations for the permanent magnet motors.

III.3. Motor Simulation Study

Computer simulation programs are being developed which will enable a direct comparison of the performance capabilities of the brushless permanent magnet machine technology versus the induction machine for various command input motion sequences. The development work has progressed using a 1.5 inch sinusoidal linear displacement as a command input for the machines. Using the provided vendor machine data, each simulation is supplied with this command input. Performance measurements of the input energy, input power, efficiency, and power loss are then obtained from the program for each motor type.

The next phase of development for these programs is to consider the impact of a motor failure on the redundant system. Since this failure could potentially occur at any time, analysis will be made of the performance response for the motors with a failure transpiring at any time within the given load cycle. Furthermore, analysis will be made assuming that the failure is a short circuiting of the stator windings. Thermal considerations will be evaluated for these scenarios with detailed analysis on temperature rise due to step torque load change and the additional heating load of the short circuited winding.

III.4. Summary

Detailed results of the simulation programs will be available in mid-March. This data should provide an adequate frame of reference to accurately evaluate the performance of the different motor options available. Hopefully, this information will also provide a reasonable perspective of how the motor performance will differ under various realistic operational load cycles. Information gathered and analysis performed for this simulation effort is also intended for publication in an appropriate technical journal.

III. References

[III.1] J.W. Mildice, "ELA/EMA Control with Resonant Power Processors", General Dynamics, Space Systems Division, September 1992.

[III.2] "Electric Thrust Vector Control for National Launch System (NLS)", Allied Signal Aerospace Company, AiResearch Los Angeles Division, September 1992.

IV. HEALTH MONITORING AND FAULT DIAGNOSIS

The health of an EMA used in a thrust vector control application must be continuously assessed. In addition, classification of EMA faults can provide data for the eventual goal of adaptive control in a fail/operate mode. For these reasons, investigation is currently underway to develop a simplistic (and thus efficient), yet accurate, scheme for performing such duties.

IV.1. System Configuration

As a starting point for our development, we assumed the form of our system that is illustrated in figure IV.1. Note that our development is focused on the estimator.

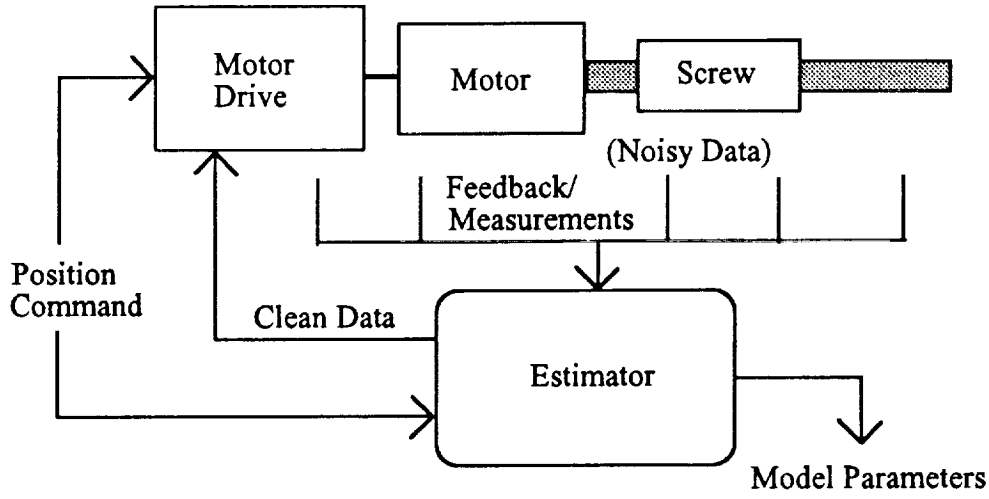

Figure IV.1. Physical System Configuration.

The estimator will receive system measurements that will inevitably contain a noise component. From this data and a system model, the estimator will filter the measurements to provide clean data to the control system. Also, the estimator will provide an estimate of multiple model parameters. The estimated model parameters will be instrumental in the detection of impending faults.

IV.2. A Test System

To begin a formal analysis, we focused solely on the EMA motor. A general dc machine model was employed. A digital simulation of the machine was written and executed. The inputs to the simulation were: armature resistance, armature inductance, torque constant, voltage constant, rotor inertia, terminal voltage, and load torque. Any of these input parameters were allowed to change at any point during simulation. The simulation was implemented with a finite-difference algorithm. The solution time step and simulation duration were user-specified.

The outputs of the simulation were: speed (ω), acceleration (α), armature current (i), terminal voltage (v), input power (p), and accelerating torque (T_a). This data represented a clean measurement set. Given the set of clean measurements, random (though controlled) noise was digitally injected into the clean data to provide a simulated set of noisy measurements. This then, formed the input data for the estimator. This "system" is illustrated in Figure IV.2.

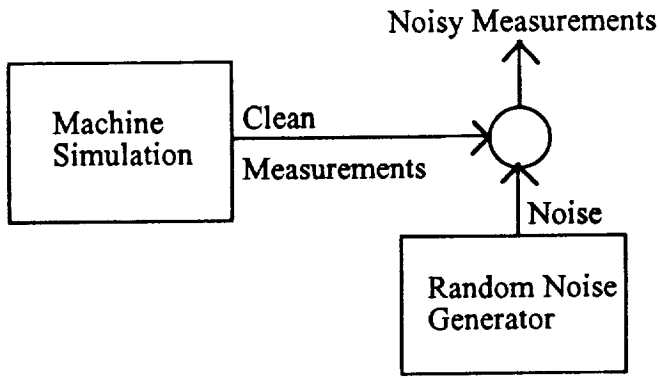

Figure IV.2. Machine/Measurement Simulator.

The derived estimator reproduced two of the measured quantities: speed and armature current. In addition, the estimator provided calculated values for the armature resistance (R) and load torque (T_L).

IV.3. Estimation Scheme

The estimation scheme chosen as the first step in this feasibility study was that of weighted-least-squares estimation. The quantities to be estimated were placed in a vector x, as shown in (IV.1). This vector is referred to as the state vector.

$$\vec{x} = [\omega \quad i \quad R \quad T_L]^T \tag{IV.1}$$

The system measurements were placed in a vector z, as shown in (IV.2). This vector is called the measurement vector.

$$\vec{z} = [\omega \quad \alpha \quad i \quad v \quad p \quad T_a]^T \tag{IV.2}$$

By using the circuit/mechanical model of the machine, each measurement was expressed as a function of state variables as indicated in (IV.3).

$$z_i = h_i(\vec{x}) \tag{IV.3}$$

The h functions were placed in a vector h. The overall objective of the estimator was to minimize the objective function J, as defined in (IV.4).

$$J = \left[\vec{z} - \vec{h}(\vec{x})\right]^T [R]^{-1} \left[\vec{z} - \vec{h}(\vec{x})\right] \tag{IV.4}$$

In (4), R is a weighing matrix that basically assigns confidence levels to each measurement. If all the measurements are assumed independent, then R will be diagonal and the i,i entry can be the statistical variance of i'th measurement.

The minimization of the objective function requires locating the specific state vector that drives the residual vector, r, to a minimal weighted value. This vector is defined in (IV.5).

$$\vec{r} = \left[\vec{z} - \vec{h}(\vec{x})\right] \tag{IV.5}$$

Since the h functions are non-linear in the state variables, this optimization requires an iterative solution. The method of choice is Newton-Raphson.

The iterative update relationship for the algorithm is presented in (IV.6). Note that the parenthetical superscripting is used to denote iteration count.

$$\vec{x}^{(k+1)} = \vec{x}^{(k)} + \left\{[G]^{-1}\right\}^{(k)} \left\{[H]^T\right\}^{(k)} [R]^{-1} \vec{r}^{(k)} \tag{IV.6}$$

In (6), the G and H matrices are the gain and Jacobian matrices, respectively. They are defined in (IV.7) and (IV.8).

$$[H]^{(k)} = \begin{bmatrix} \nabla h_1^T\left(\vec{x}^{(k)}\right) \\ \nabla h_2^T\left(\vec{x}^{(k)}\right) \\ \cdot \\ \cdot \\ \cdot \\ \nabla h_m^T\left(\vec{x}^{(k)}\right) \end{bmatrix} \tag{IV.7}$$

$$[G]^{(k)} = \left\{[H]^T\right\}^{(k)} [R]^{-1} [H]^{(k)} \tag{IV.8}$$

In (IV.7), m is the number of measurements.

Convergence is detected when the residual vector comes within a predetermined tolerance. Also, the final value of the objective function gives information as to the accuracy of the fit. For a hardware implementation, the number of iterations must be fixed at a predetermined value. The existence of the inverse of the gain matrix guarantees system observability.

Several of the h functions involved differential equations. In these instances, a first order finite-difference approximation to the derivative was employed. The dependence

on the value of the state variable at the previous solution point was taken as a constant computed from the previous state estimate.

IV.4. Initial Results

To determine the feasibility of the proposed algorithm, a set of dc machine parameters was chosen. The data is provided in Table IV.1.

Table IV.1. Machine Data.

Quantity	Value	Units
Armature Resistance	0.1	Ω
Armature Inductance	20	mH
EMF/Torque Constant	1.45	Vs/rad or N-m/A
Moment of Inertia	0.8	kg-m^2
Terminal Voltage	260	V
Load Torque	203.5	N-m

Three specific tests were performed. In all tests, the simulation began at starting and ran for a total simulation time of 3 seconds. Each case will be presented individually.

IV.4.1. Case 1

For the first test, no disturbance was applied to the system. However, random noise of up to 20% of the actual value was injected into the armature current measurement. Figure IV.3 shows the actual current, the noisy current measurement, and the estimate of the current. The estimate substantially reduced the large noise component.

IV.4.2. Case 2

The case 2 scenario included a random noise component of up to 10% injected to the armature current measurement as a random noise component of up to 5 N-m injected into the accelerating torque measurement. Figure IV.4 displays the estimator tracking the armature current. Figure IV.5 illustrates the noise component on the accelerating torque, and Figure IV.6 shown the actual and estimated values of load torque. Here again, the estimator performed quite well.

IV.4.3. Case 3

For the final study case included here, a system disturbance was introduced. A step change in the load torque from 203.5 N-m to 50.875 N-m was applied at 1.55 seconds. The armature current measurement received a random noise injection of up to 20% of the actual value. Figures IV.7 and IV.8 illustrate the estimator tracking of the armature current and load torque, respectively. The results are quite favorable.

Figure IV.3. Motor Current.

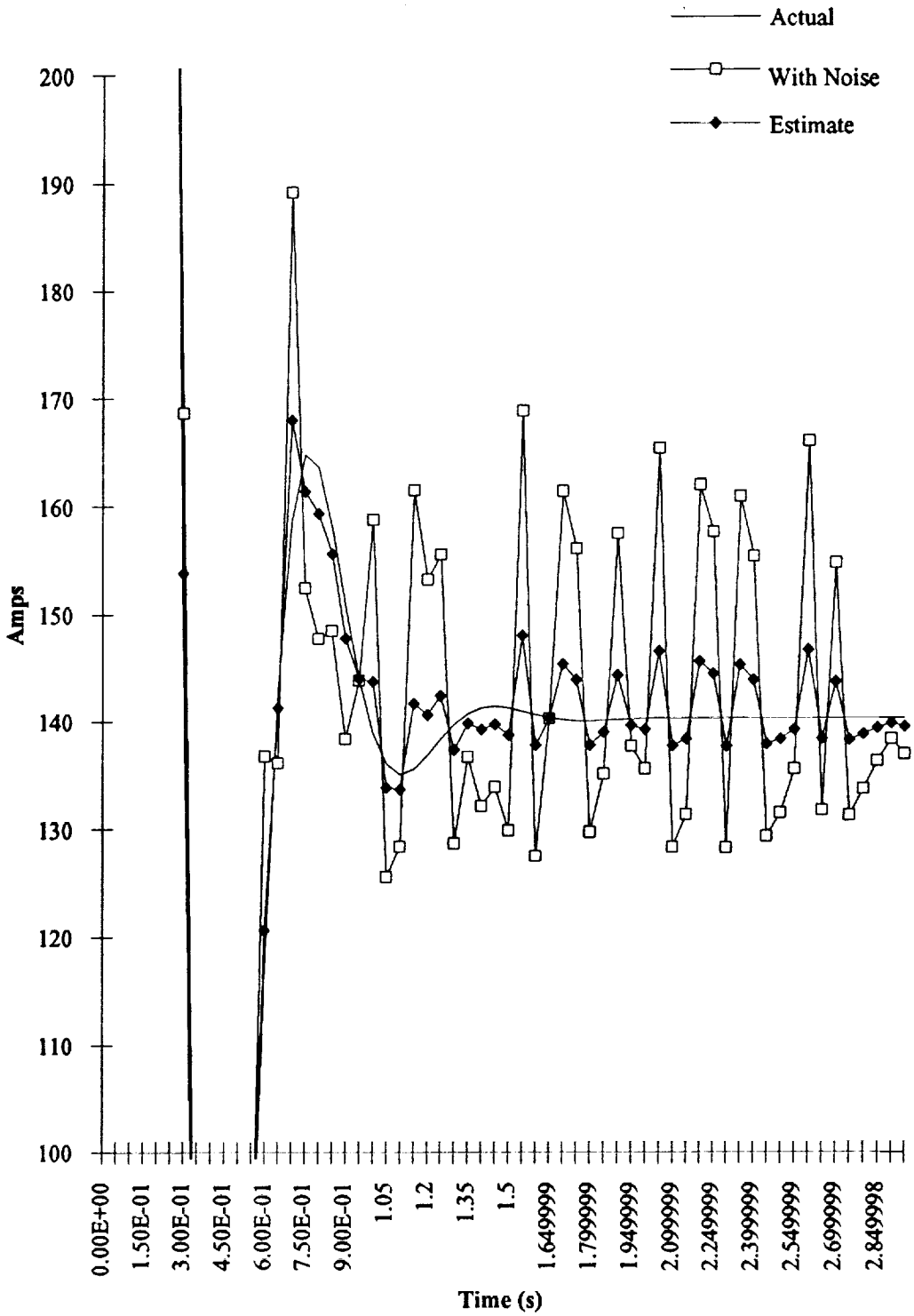

Figure IV.4. Motor Current.

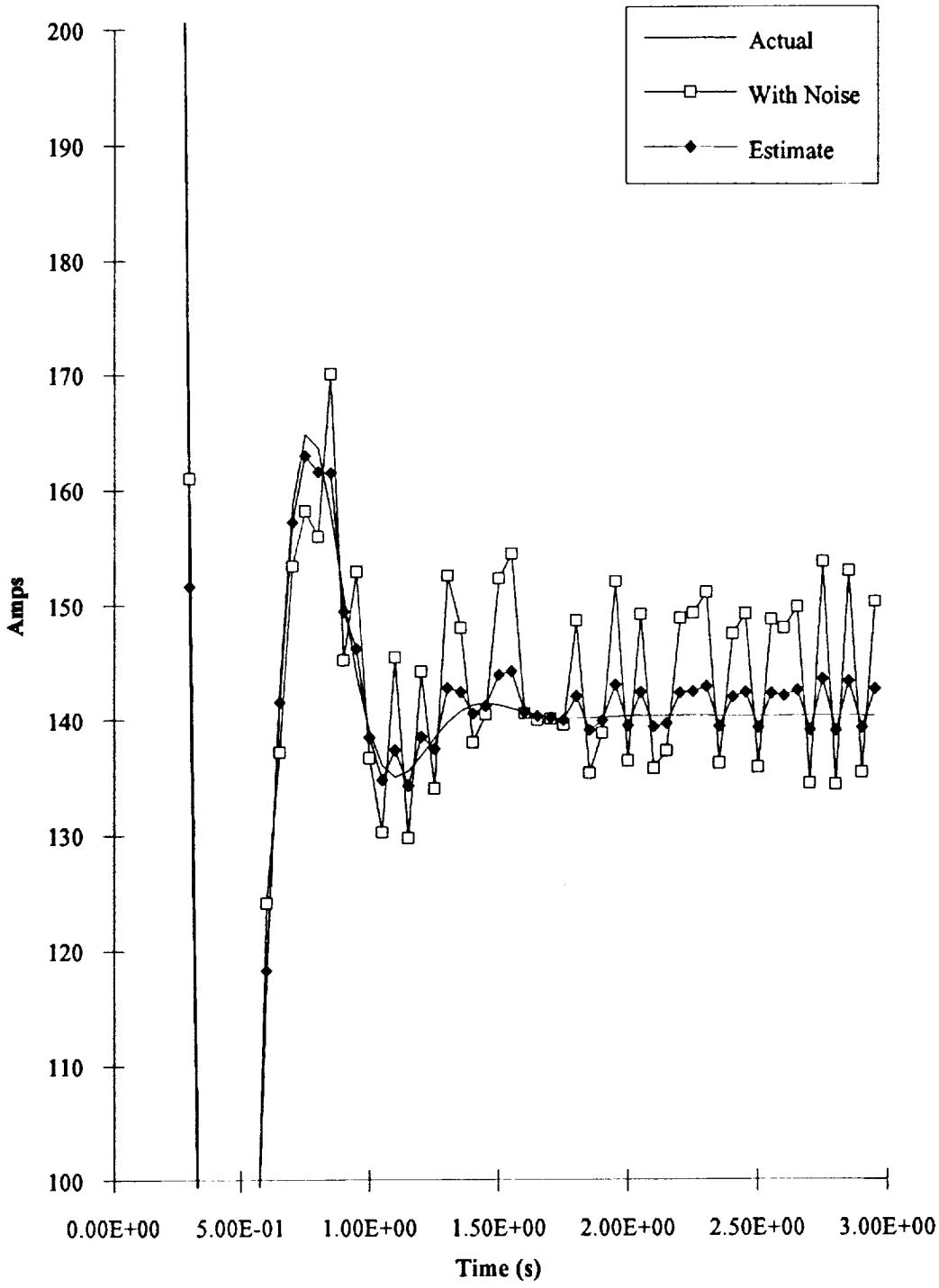

Figure IV.5. Accelerating Torque.

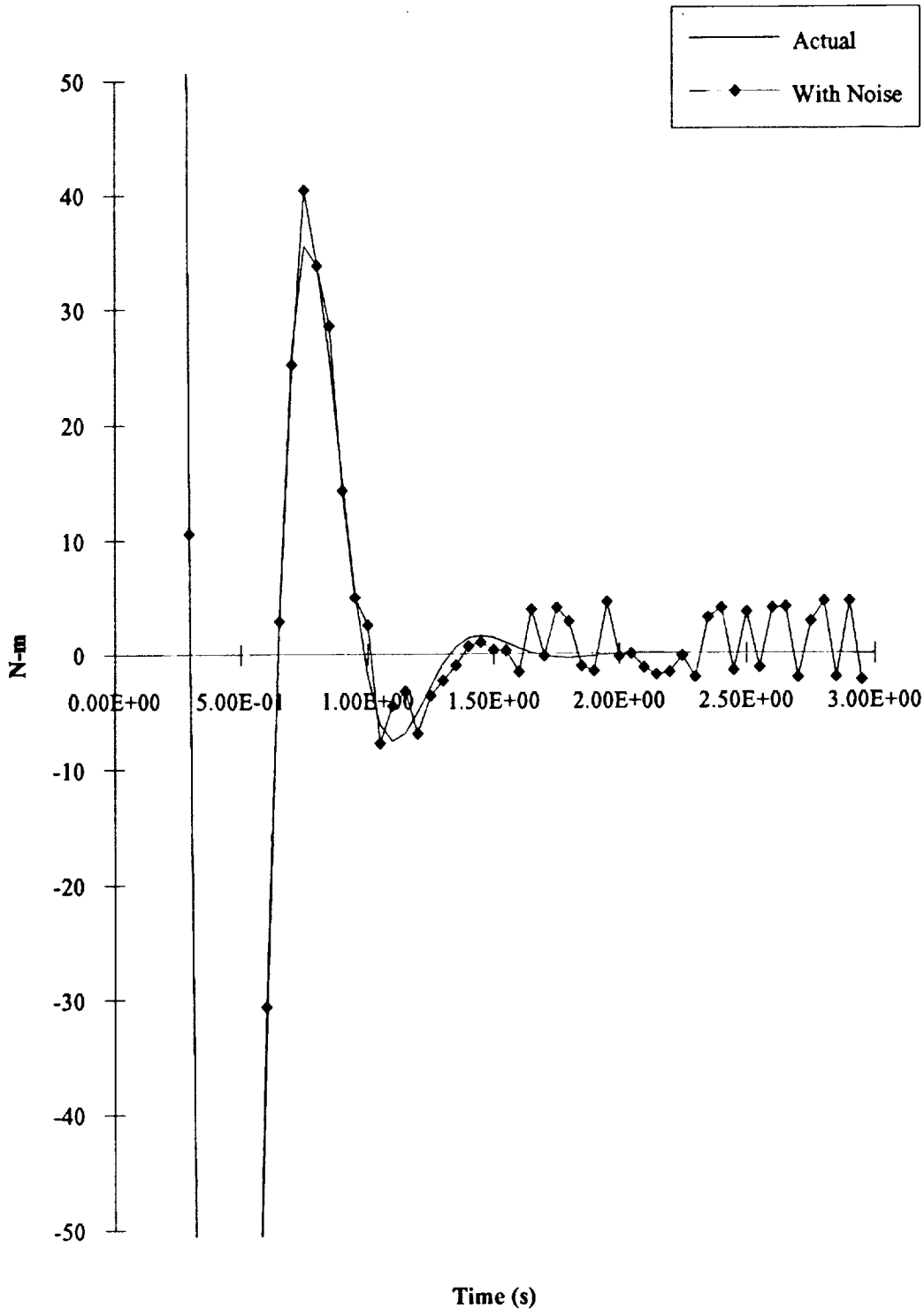

Figure IV.6. Load Torque.

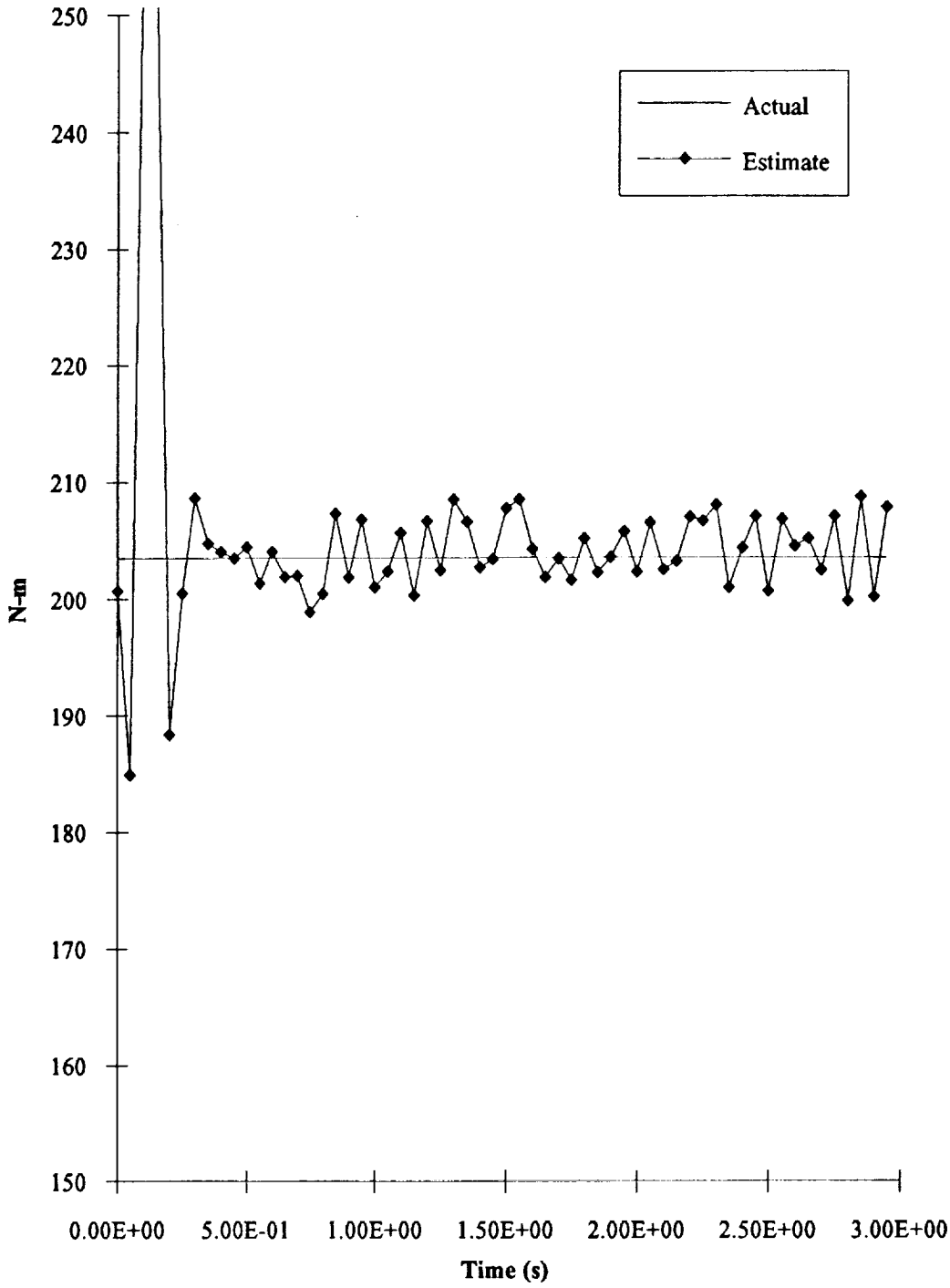

Figure IV.7. Motor Current.

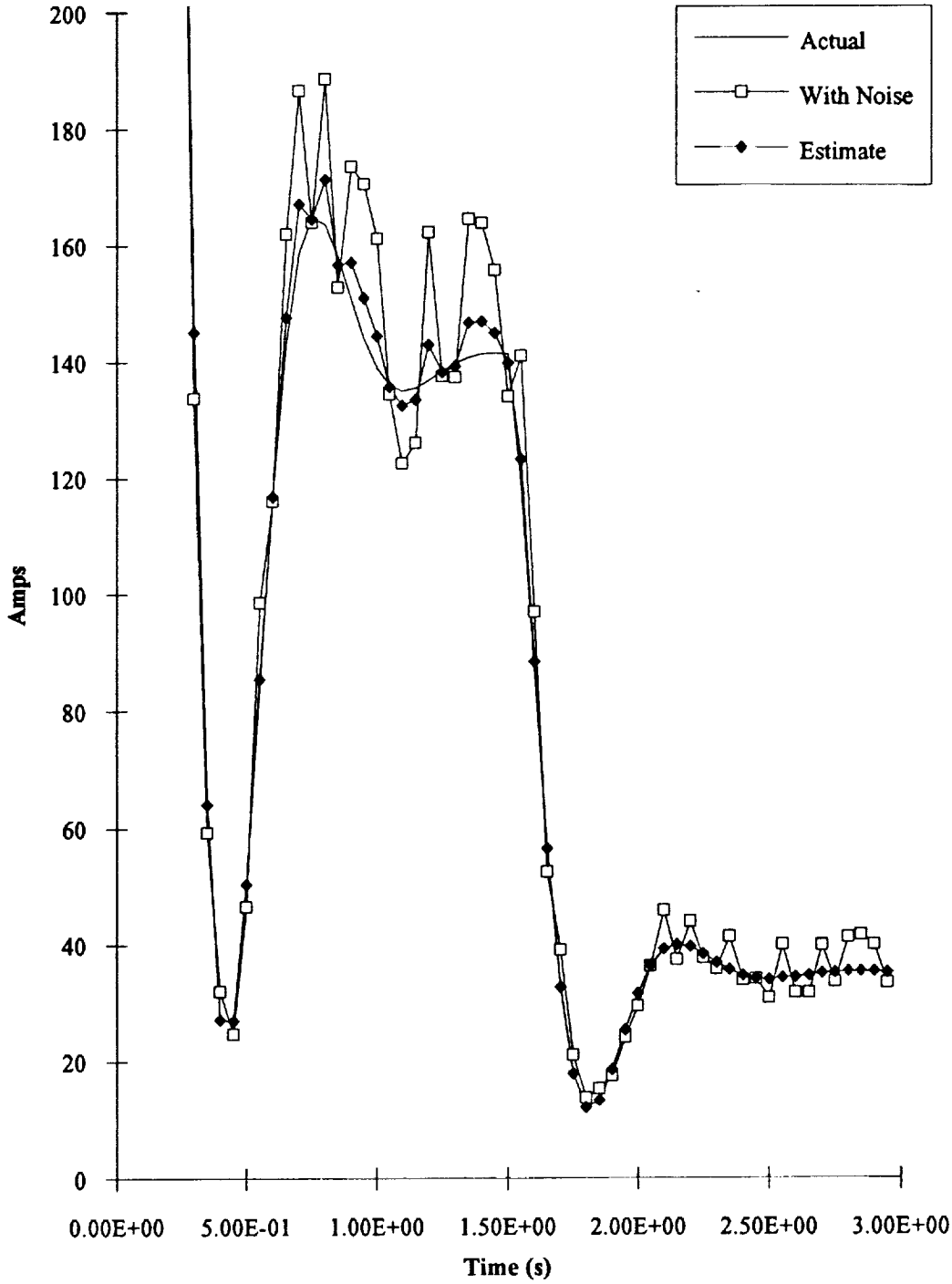

Figure IV.8. Load Torque.

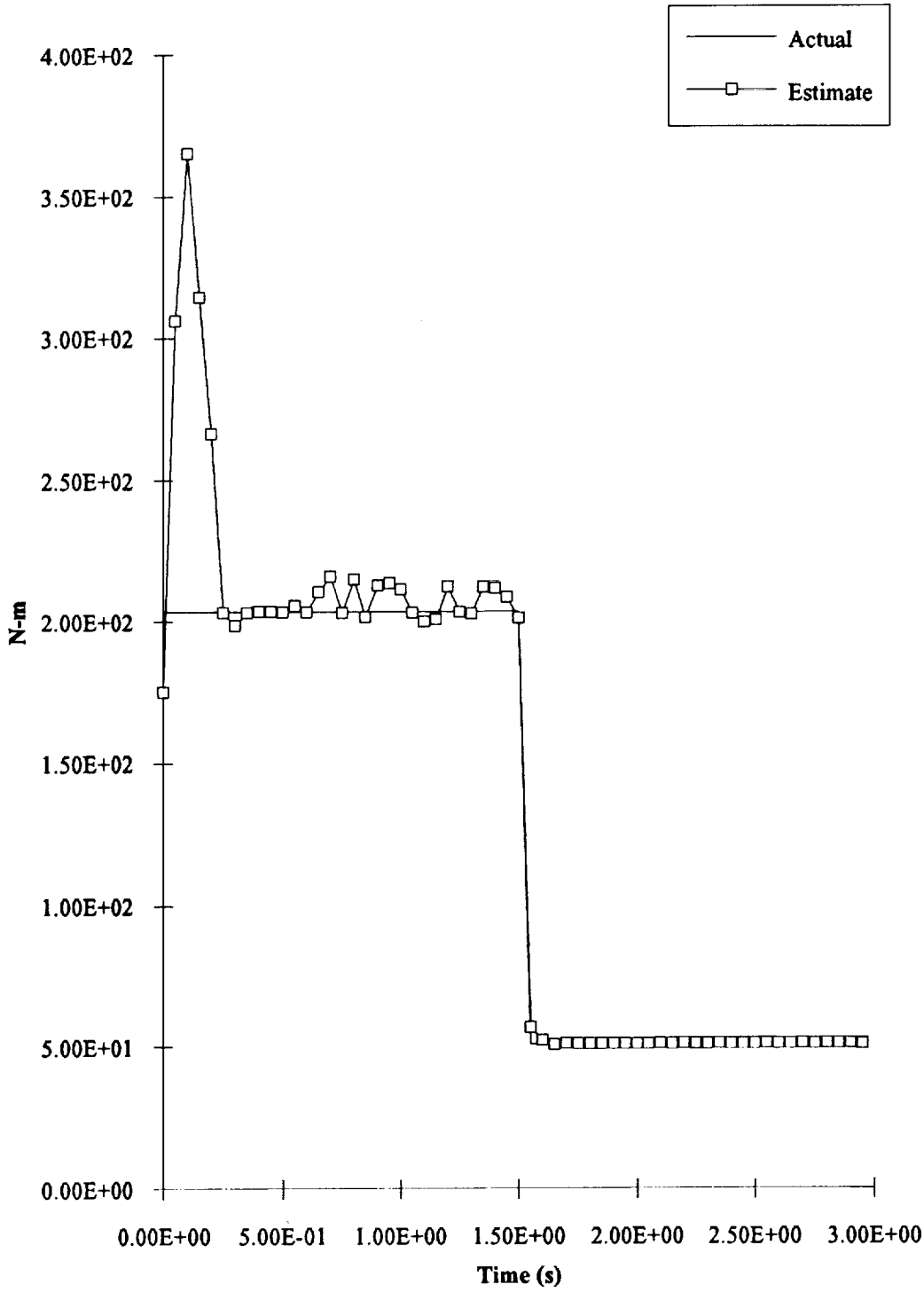

IV.5. Laboratory Facilities

The Department of Electrical Engineering currently maintains a configurable machine in a laboratory environment. Various rotor and stator configurations can easily be assembled to provide a variety of different machine topologies. In addition, the shaft of this machine is coupled to a controllable load. All of this equipment was manufactured by Feedback Instruments, Limited.

In the same laboratory, a PC controlled data acquisition system is available. We are currently interfacing the data acquisition system with the machine set. Our goal is to gather actual data and verify estimator results in the lab. We would also like the opportunity to do similar work with the actuator at MSFC.

IV.6. Summary

At this point in our work, we feel certain that a standard estimation package will be quite sufficient and effective to perform health monitoring and fault diagnosis on electromechanical actuators for thrust vector control applications. Efforts are currently underway to apply the algorithm presented here as well as standard Kalman filtering techniques to the entire actuator system including the motor drive, motor, and screw.

The results produced to date indicate several areas that will require further study. One area is the possible use of data scaled into per-unit quantities. Perhaps the obvious choice will be to scale the data to the range of the sensors used for measurement. The per-unit approach has proven to provide substantially more accurate results for similar state estimation problems in the electric utility industry.

Additionally, we feel that the use of a highly effective estimation algorithm may eliminate the need for some system measurements. The final determination of this fact will rely heavily on a failure mode study, however. Along with this fact, we can also see substantial advantages to utilizing estimator outputs as control system feedback rather

than actual measurements. This will certainly be advantageous in high accuracy applications.

Perhaps one of the major advantages of the presented estimation approach is that residual analysis provides a great deal of information on sensor error. Failed or faulty sensors are easily detected. If sufficient redundancy is present in the measurement scheme, for the sake of observability, then failed sensor outputs can easily be ignored. Note that the requirement of redundancy is focused on the question of observability. Thus, redundancy in this context does not imply an identical measurement or sensor.

While our developments to date are entirely software oriented, we feel that a final algorithm can be readily implemented in hardware. Such an implementation could and would operate at extremely high speeds. In fact, we anticipate that a special purpose estimation "chip" would not introduce any significant time lag in the control loop. However, fault diagnosis and residual analysis would. Thus, we suggest that these algorithms, which would require input from the estimator, would be better executed off-line at a ground-based facility.